Resonant Charging Performance of Spiral Tesla Transformer Applied in Compact High-Voltage Repetitive Nanosecond Pulse Generator

Yunlong Liu, Li Lee, Yu Bing, Yafeng Ge, Wen Hu, and Fuchan Lin

***Abstract*— The compact, small-sized device based on a pulsed transformer combined with a semiconductor switch is a feasible solution that generates the high-frequency and high-voltage pulse. Compared with other types of transformers, spiral Tesla transformer is much easier to achieve a high output-voltage ratio. By an in-depth analysis of the resonance circuit of Tesla transformer, the expressions of secondary voltage, transformation ratio, peak, and steepness of the primary current are deduced and analyzed in this paper. The development test of a small-size Tesla transformer prototype has been performed. The key electrical characteristics are further measured, estimated, and discussed. The specification parameter selection of the primary semiconductor switch must rely on the characteristics of primary current. Applied to a 6.0 kΩ resistor, the high-voltage repetitive pulse generator based on the Tesla transformer prototype can generate a series of pulses with a peak voltage of 100 kV and a rise time of 40 ns at the repetition rate of 200 Hz. Atmospheric air nonequilibrium plasma can be formed using the developed pulse generator and some typical images are presented.**

***Index Terms*— Dielectric barrier discharge, repetitive nanosecond pulse, resonant charging, Tesla transformer, thyristor.**

I. Introduction

THE explorations on dielectric insulation and electric discharge phenomena with nanosecond pulse have developed into an active focal point of new technology on electrical engineering [1]–[3]. High-voltage nanosecond pulse generator (HVNPG) also has very extensive applications, such as multiple switch synchronous triggering, ultrawide band system (UWB), dielectric barrier discharge (DBD), food sterilization, waste gas and water treatment, ozone making, material surface modification, and ultraviolet source [4]–[9].

With a technical progress, the need for a pulsed power source, which is compact, portable, and highly reliable, is increasing currently. The RADAN series HVNPG developed by the Institute of High Current Electronics in Russia represents the higher level in this field [10]. The combination of transient pulsed transformer and semiconductor switch is an effective way to realize the HVNPG [10]–[15]. There are two main types of pulse transformers: Tesla transformer and magnetic core transformer. A Tesla transformer transfers energy through magnetic coupling between primary and secondary windings without magnetic core. Therefore, the coupling coefficient of the Tesla transformer is generally less than that of the magnetic core transformer. However, exactly for the same reason, energy coupling of Tesla transformer does not suffer from the limitation of saturation and frequency dependence of ferromagnetic material [16], [18]. Tesla transformer is mainly comprised of two types: tape helix and spiral. Compared with the former, spiral Tesla transformer has the advantages of simple construction, small turn-to-turn capacitance, low cost, easiness to achieve a high transformation ratio, and so on [18]. The high transformer ratio can ensure that the charging voltage is low enough so that controllable semiconductor devices, such as thyristor, can be used as a primary switch [15]–[19], which is easy to achieve high repetition rate and has more applications.

When working in the resonant state where the primary and the secondary intrinsic frequencies are equal, a Tesla transformer can attain the maximum efficiency and high transformation ratio [20], [21]. The output voltage and transformation ratio are very important in the resonant charging characteristics of a Tesla transformer. Moreover, spiral Tesla transformer is usually with a single-turn primary winding so that its magnetizing inductance is very small. Accordingly, the primary current of a Tesla transformer is generally greater than that of a magnetic core transformer. This speciality is very demanding for the semiconductor switch used in the primary side.

Combined with the practical application in this paper, the resonant charging characteristics of spiral Tesla transformer has been in-depth studied. Based on the resonance charging model, the arithmetic expressions for secondary voltage, transformation ratio, primary current, and its maximum rise-rate were deuced. One small-sized spiral Tesla transformer prototype has been constructed too. The characteristics of the key parameters were further studied through experiment in detail. Then, the rise-rate of turn-on current of the primary semiconductor switch has been discussed. Utilizing the sharpening switch after secondary capacitance, the HVNPG based on the Tesla transformer is capable of delivering, to a 6.0 kΩ resistor, an output pulse of 100 kV in a peak voltage with a rise

Manuscript received April 11, 2013; revised August 12, 2013 and August 30, 2013; accepted October 9, 2013. Date of publication October 30, 2013; date of current version December 9, 2013. This work was supported in part by the National Natural Science Fund, China, under Grant 51107049 and in part by the Independent Innovation Research Fund of HuaZhong University of Science and Technology under Grant 2013KXYQ002.

The authors are with the State Key Laboratory of Advanced Electromagnetic Engineering and Technology, Huazhong University of Science and Technology, Wuhan 430074, China (e-mail: 772678472@qq.com; leeli@mail.hust.edu.cn).

Color versions of one or more of the figures in this paper are available online at http://ieeexplore.ieee.org.

Digital Object Identifier 10.1109/TPS.2013.2285782

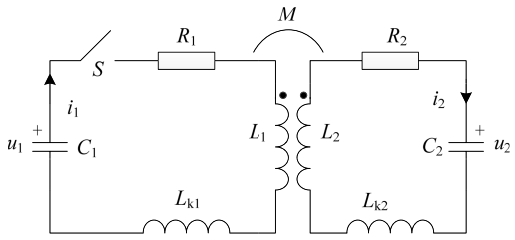

Fig. 1. Resonant model of Tesla transformer.

time of 40 ns at the repetition rate of 200 Hz. The conclusions from this paper can be used as a reference for the development of the compact HVNPG based on the Tesla transformer.

II. Analysis of Resonant Circuit

As shown in Fig. 1, the circuit model of the Tesla transformer involves two air-coupled, damped resonant circuits. C_1 is the primary capacitor. L_1 and R_1 are the equivalent inductor and resistor of the primary winding, respectively. L_{k1} is the stray inductance of the primary side. The corresponding elements of the secondary side are marked up as C_2, L_2, R_2, and L_{k2}. M denotes the mutual inductance. After C_1 is charged for a defined voltage by the dc supply, through a controllable switch S, C_1 discharges to the primary winding. Afterwards, an oscillating high-voltage across C_2 will be obtained.

Since the magnetizing inductance of an air core Tesla transformer is small, the equivalent circuit should obey the dual-loop equations. According to the first Kirchhoff law, the differential equations are

$$(L_1 + L_{k1})\frac{di_1}{dt} + \frac{1}{C_1}\int i_1\,dt - M\frac{di_2}{dt} + R_1 i_1 = 0 \quad (1)$$

$$(L_2+L_{k2})\frac{di_2}{dt} + \frac{1}{C_2}\int i_2 dt - M\frac{di_1}{dt}+R_2 i_2 = 0. \quad (2)$$

To solve the above equations, some new parameters may be introduced. k_{eff} and n_{eff} are the effective coupling coefficient and effective turns ratio, while ω_{01} and ω_{02} are the angular resonance frequencies of the uncoupled primary and secondary circuits, respectively. In addition, Q_1 and Q_2 are the quality factor of primary and secondary circuits.

Introducing the differential operation with respect to time t and substituting the new parameters into (1) and (2) and after rearranging, the equations will change to

$$\frac{d^2 i_1}{dt^2} + \frac{\omega_{01}}{Q_1}\frac{di_1}{dt} + \omega_{01}^2 i_1 = \frac{M}{L_1 + L_{k1}}\frac{d^2 i_2}{dt^2} \quad (3)$$

$$\frac{d^2 i_2}{dt^2} + \frac{\omega_{02}}{Q_2}\frac{di_2}{dt} + \omega_{02}^2 i_2 = \frac{M}{L_2 + L_{k2}}\frac{d^2 i_1}{dt^2} \quad (4)$$

where

$$\omega_{01}^2 = \frac{1}{(L_1 + L_{k1})C_1} \quad \omega_{02}^2 = \frac{1}{(L_2 + L_{k2})C_2} \quad (5)$$

$$Q_1 = \frac{\omega_{01}(L_1 + L_{k1})}{R_1} \quad Q_2 = \frac{\omega_{02}(L_2 + L_{k2})}{R_2} \quad (6)$$

$$k_{\text{eff}}^2 = \frac{M^2}{(L_1 + L_{k1})(L_2 + L_{k2})} \quad n_{\text{eff}}^2 = \frac{L_2 + L_{k2}}{L_1 + L_{k1}}. \quad (7)$$

Let us α define α as a detuning coefficient that indicates the resonant condition

$$\alpha = \omega_{02}^2 \Big/ \omega_{01}^2. \quad (8)$$

If $\alpha = 1$, this will mean the idea resonance of the primary and the secondary sides.

Equations (3) and (4) form 2 by 2 equations whose characteristic equation is a fourth-order linear homogeneous differential equation. Suppose the complex roots are $\{j\omega_m\}$, $m = 1, 2, 3, 4$, the general solutions of these 2 by 2 equations are

$$i_1(t) = \sum_{m=1}^{4} A_m e^{j\omega_m t}, \quad m = 1, 2, 3, 4 \quad (9)$$

$$i_2(t) = \sum_{m=1}^{4} B_m e^{j\omega_m t}, \quad m = 1, 2, 3, 4. \quad (10)$$

The constants A_m and B_m are two undetermined coefficients related to the initial conditions. Let $x_m = \omega_m/\omega_p$ and $\omega_p = \omega_{02}$. ω_p is the resonant frequency of a Tesla transformer and (9) and (10) are substituted into (3) and (4). After multiplying the two corresponding sides of the equations, the following equation will be obtained:

$$\left(x_m^2 - j\frac{1}{Q_1\sqrt{\alpha}}x_m - \frac{1}{\alpha}\right)\left(x_m^2 - j\frac{1}{Q_2}x_m - 1\right) = k_{\text{eff}}^2 x_m^4. \quad (11)$$

In an ideal case with $R_1 = R_2 = 0$ and $Q_1 = Q_2 = 0$, the fourth-order characteristic equation will change into a two second-order one, and the expression of x_m is readily solved as

$$x_{\pm}^2 = \frac{1+\alpha}{2\alpha\left(1 - k_{\text{eff}}^2\right)}\left[1 \pm \sqrt{1 - \frac{4\alpha\left(1 - k_{\text{eff}}^2\right)}{(1+\alpha)^2}}\right]. \quad (12)$$

Let $\omega_1^2 = x_+^2\omega_p^2$, $\omega_2^2 = x_-^2\omega_p^2$ and the constants A_m and B_m can be evaluated by the initial conditions, i.e., $u_1(0) = U_0$, $u_2(0) = 0$, $i_1(0) = 0$, $i_2(0) = 0$. Therefore, the expressions of primary current i_1 and secondary voltage u_2 are

$$i_1(t) = -U_0 C_1 \omega_1 \frac{x_-^2\left(x_+^2 - 1\right)}{x_+^2 - x_-^2} \times \left[\sin\omega_1 t + \frac{x_+\left(1 - x_-^2\right)}{x_-\left(x_+^2 - 1\right)}\sin\omega_2 t\right] \quad (13)$$

$$u_2(t) = U_0\frac{C_1 k_{\text{eff}}}{C_2 n_{\text{eff}}}\frac{x_-^2 x_+^2}{x_+^2 - x_-^2}[\cos\omega_1 t - \cos\omega_2 t]. \quad (14)$$

Substituting (3), (5), and (10) into (16), it is obtained that

$$u_2(t) = U_0 n_{\text{eff}} V(\cos\omega_1 t - \cos\omega_2 t) \quad (15)$$

where

$$V = \alpha k_{\text{eff}} \Big/ \sqrt{(1+\alpha)^2 - 4\alpha\left(1 - k_{\text{eff}}^2\right)}. \quad (16)$$

Actually, because the values of R_1 and R_2 cannot be neglected, the effect of R_1 and R_2 can be regarded as a damped portion of the secondary voltage [16] as follows:

$$u_2(t) = U_0 n_{\text{eff}} V e^{-t/T}(\cos\omega_1 t - \cos\omega_2 t) \quad (17)$$

where the damping time constant is

$$T = \frac{4(L_1 + L_{k1})(L_2 + L_{K2})}{R_2(L_1 + L_{k1}) + R_1(L_2 + L_{K2})}\left(1 - k_{\text{eff}}^2\right). \quad (18)$$

Because L_2 is much larger than L_1, (18) can be simplified as

$$T = \frac{4(L_1 + L_{k1})}{R_1}\left(1 - k_{\text{eff}}^2\right). \quad (19)$$

The actual transformation ratio is defined as

$$\lambda = \left|\frac{(u_2)_{\max}}{U_0}\right| = n_{\text{eff}} V e^{-t_{\max}/T} \delta_{\max} \quad (20)$$

where $\delta_{\max}$ is the maximum value of $(\cos \omega_1 t - \cos \omega_2 t)$ at the moment $t_{\max}$.

Equation (16) indicates that the secondary voltage u_2 of the Tesla transformer consists of two cosine waves with different frequencies. Numerous studies show that the time when u_2 reaches its maximum value, $(u_2)_{\max}$ is mainly influenced by an effective coupling coefficient k_{eff} [15]–[18]. When $k_{\text{eff}} > 0.8$, $(u_2)_{\max}$ is at the first peak value of u_2; however, when k_{eff} approaches to 0.6, $(u_2)_{\max}$ arrives at the second peak value of u_2. The design and construction of air-core Tesla transformer, whose effective coupling coefficient is larger than 0.8, are very difficult. Therefore, $(u_2)_{\max}$ has been at the second peak generally [16], [18], and the transformation ratio λ can be calculated by the ratio of the second peak value of u_2 and the charging voltage U_0. From (16) and (17), it can be concluded that the voltage ratio λ will be determined by k_{eff}, n_{eff}, $L_1 + L_{k1}$, R_1, and V that represent the impact of the resonance on $(u_2)_{\max}$ and λ.

The spark gap is usually selected as the primary switch S in the early Tesla transformers. With the development of power semiconductor technology, the spark gap can be replaced by a controllable semiconductor switch, so that the more compact structure can be achieved. However, the existing semiconductor switches have some severe limitations not yet overcome in applications that are for high voltage, great current and fast rise-rates. Generally, high transformation ratio can be easily achieved in the spiral Tesla transformer, which guarantees that the charging voltage U_0 will not be too high. Therefore, for the Tesla transformers, the possibility using semiconductor switch should mainly rely on the maximum value and rise-rate of current across the primary circuit.

During the resonant state, i.e., $\alpha = 1$, from (12) and (13), the primary current i_1 can be expressed as

$$i_1(t) = \frac{-U_0 C_1 \omega_1}{2}\left[\sin\,\omega_1 t + \sqrt{\frac{1 - k_{\text{eff}}}{1 + k_{\text{eff}}}}\sin \omega_2 t\right]. \quad (21)$$

Because the $\omega_1 > \omega_2$, the primary current i_1 will reach its peak value $(i_1)_{\max}$ when $\sin \omega_1 t = 1$. Hence $(i_1)_{\max}$ can be expressed as

$$(i_1)_{\max} = \frac{-U_0\sqrt{C_1}}{2\sqrt{(1 - k_{\text{eff}})(L_1 + L_{k1})}} \times \left[1 + \sqrt{\frac{1 - k_{\text{eff}}}{1 + k_{\text{eff}}}}\sin\left(\frac{\pi}{2}\sqrt{\frac{1 - k_{\text{eff}}}{1 + k_{\text{eff}}}}\right)\right]. \quad (22)$$

From (21), the maximum rise-rate of the primary current, $(di_1/dt)_{\max}$, also can be obtained as

$$\left(\frac{di_1}{dt}\right)_{\max} = \frac{U_0}{(1 - k_{\text{eff}}^2)(L_1 + L_{k1})}. \quad (23)$$

As shown in (22), since U_0 is fixed, $(i_1)_{\max}$ should be proportional to $\sqrt{C_1}$, and inversely proportional to $L_1 + L_{k1}$. According to (23), $(di_1/dt)_{\max}$ across the primary switch is also inversely proportional to $L_1 + L_{k1}$. Both $(i_1)_{\max}$ and $(di_1/dt)_{\max}$ are all influenced by k_{eff}, and the parameters k_{eff}, L_1, and L_{k1} depend on an actual transformer. When the Tesla transformer has been constructed, the value of k_{eff}, L_1, L_{k1} will be fixed. Thus $(i_1)_{\max}$ and $(di_1/dt)_{\max}$ can be simplified as the linear relation expressions

$$(i_1)_{\max} = \gamma U_0\sqrt{C_1} \quad (24)$$

$$(di_1/dt)_{\max} = \eta U_0 \quad (25)$$

where γ and η can be calculated by theoretical arithmetic or experimental data at the low voltage.

III. Experiments

Serving as a high-voltage transient transformer, from the foregoing analyses, it can be known that the charging characteristics of the Tesla transformer are notably influenced by parameters such as primary resistance R_1, stray inductance L_{k1}, and effective coupling coefficient k_{eff}. However, these parameters were associated with the device structure and workmanship and cannot totally rely on the theoretical calculation to obtain the specific value. These causes determine that the experiment study is necessary in the research of Tesla transformer.

A. Experimental Prototype

A compact spiral Tesla transformer has been prototyped. The maximum value of charging voltage had to be reduced to 1.0 kV, so that a fast switching thyristor can be used as the primary switch. The transformation ratio should be more than 100 when the expectable $(u_2)_{\max}$ is closed to 100 kV.

As shown in Fig. 2, the overall structure of Tesla transformer consists of two coaxial hollow nylon cylinders. The primary winding, made of wide copper of thickness 0.2 mm, is fixed on the outer surface of the larger (external) cylinder by an insulation glue. The material of secondary winding is polyester-enamelled wire, with the outer diameter of 0.22 mm, which is closely wound on the outer surface of the smaller (internal) cylinder. To prevent from becoming loose, the secondary winding is also fixed by the insulation glue. Two nylon cylinders are fixed coaxially and two windings are grounded together. The high-voltage terminal of the secondary winding connects C_2 through high-voltage wire. The insulation between the primary and the secondary windings is mainly provided by the wall of the external cylinder, whose thickness is 10 mm. The weight of the transformer prototype is 1.9 kg. The detailed structural data have been shown in Table I, where l is the height of winding, and r_1, r_2, and N_1, N_2 are the radius and turns number of the primary and secondary windings, respectively.

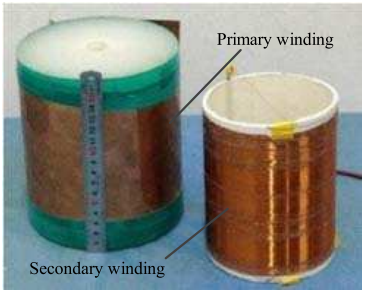

Fig. 2. Two nylon cylinders of Tesla transformer prototype.

TABLE I
STRUCTURAL PARAMETERS OF TESLA TRANSFORMER

Parameters	l (mm)	$2r_1$ (mm)	$2r_2$ (mm)	N_1	N_2
Values	130	140	110	1	480

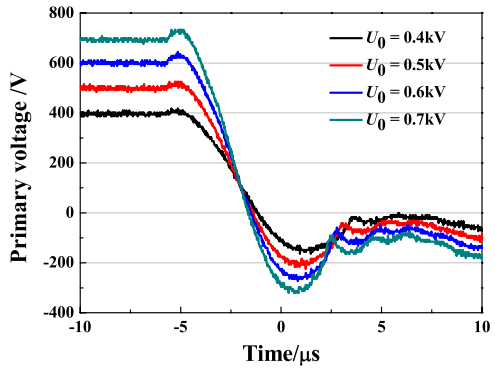

Fig. 3. Waveforms of primary voltage $u_1(t)$ with different U_0.

B. Experimental Results Analysis

As the stray inductance L_{k1} was unknown, (3) shows that the resonance degree of Tesla transformer cannot be calculated precisely. C_1 and C_2 will be changed to study the charging characteristics with the different resonance degrees in the experiment. The primary capacitor C_1 is charged by a half-wave rectification and the primary switch S is a controllable fast switching thyristor. The measurements are performed by a Tektronix TDS2024B oscilloscope, a Tektronix high-voltage probe P6015A, and a Pearson Model 110 current transformer with 10× attenuator.

When $C_1 = 10$ μF and $C_2 = 100$ pF, the waveforms of the primary voltage u_1 and secondary voltage u_2 are shown in Figs. 3 and 4, respectively. In Fig. 5, the waveform of primary current i_1 has also been shown. Fig. 4 proves that the maximum value of u_2 reaches at the second peak. In Fig. 5, when the primary voltage was only 0.7 kV, $(i_1)_{\max}$ had exceeded 3.0 kA, and the mean rise-rate, $(di_1/dt)_{\text{mean}}$, had been close to 0.6 kA/μs. It is a remarkable feature of the Tesla transformer that $(i_1)_{\max}$ and di_1/dt are all terribly large, compared with that of the magnetic core transformer.

When C_2 increased from 100 pF to 200 pF and U_0 was maintained at 0.6 kV, the variation trend of the transformation ratio λ is shown in Fig. 6. It can be observed in Fig. 6 that λ

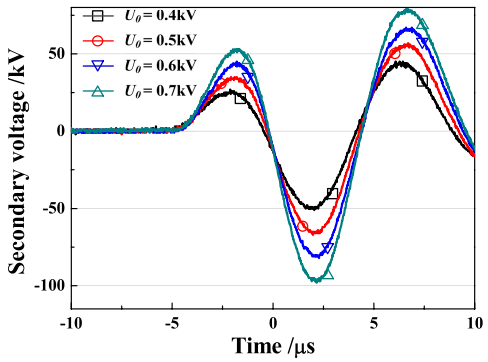

Fig. 4. Waveforms of secondary voltage $u_2(t)$ with different U_0.

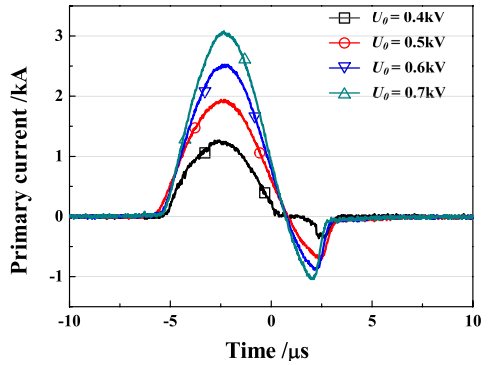

Fig. 5. Waveforms of primary current $i_1(t)$ with different U_0.

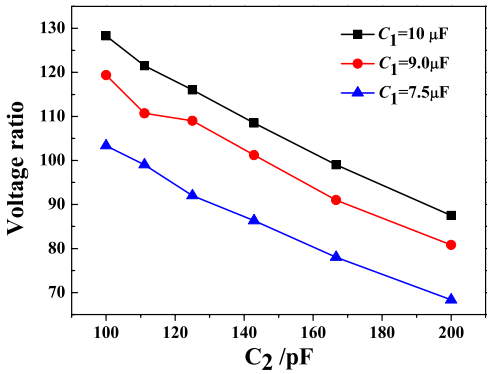

Fig. 6. Voltage ratio λ with different C_2 when $U_0 = 0.6$ kV.

declined linearly with the increasing of C_2, while λ increased with C_1 same as C_2. Equations (5) and (8) represent that the different C_1 and C_2 will result in the different detuning coefficients. Therefore, the conclusion is that the larger α will mean the higher λ.

Accordingly, it is known that α will only depend on C_2/C_1 because (L_1+L_{k1}) and (L_2+L_{k2}) are mainly fixed for a ready-made Tesla transformer. If C_2/C_1 is kept at constant, which means α was stable, the experimental relationship between λ and U_0 with different C_1 and C_2 is plotted as shown in Fig. 7. It can be seen that λ increased with C_1 even if the values of both α and C_2/C_1 kept stable. However, as shown in (17) and (20), u_2 and λ are related with α and C_2/C_1 while have nothing with the specific values of C_1 and C_2. The reason that experimental results were not in conformity with the analysis

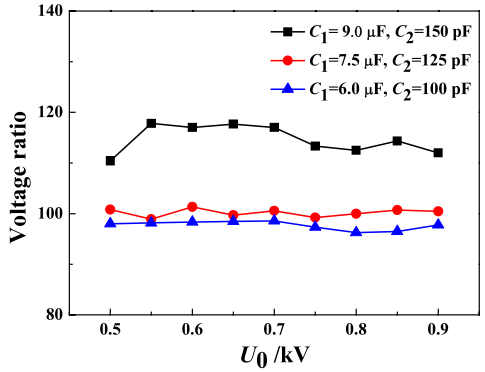

Fig. 7. Voltage ratio λ with different U_0.

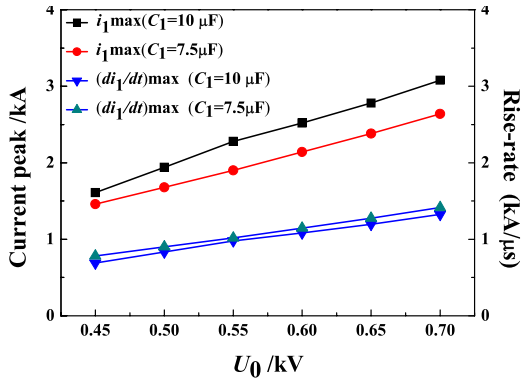

Fig. 8. Maximum values of primary current and its rise-rate.

TABLE II
MEASURED VALUES OF L_1, L_2, R_p, AND R_s

f (kHz)	L_1 (nH)	L_2 (mH)	R_p (mΩ)	R_s (Ω)
100	96.20	14.27	1.86	65

of (17) and (20) could be that the greater C_1 has aroused the greater primary current and the increasing of primary current may enhance the transformer coupling.

When C_2 kept at 100 pF, and C_1 was 10 μF and 7.5 μF, the change rules of $(i_1)_{\max}$ and $(di_1/dt)_{\max}$ are shown in Fig. 8. $(di_1/dt)_{\max}$ were calculated according to the method proposed in [22], i.e., $(di_1/dt)_{\max}$ equals $\pi/2$ times $(di_1/dt)_{\text{mean}}$. As shown in Fig. 8, both $(i_1)_{\max}$ and $(di_1/dt)_{\max}$ increase linearly with charging voltage, and $(i_1)_{\max}$ is sensitive to the change of C_1, while $(di_1/dt)_{\max}$ was not.

C. Further Analysis of Key Parameters

Equations (5), (16), (19), and (20) show that the resistance R_1 and stray inductance L_{k1} have a big impact on the voltage and current of Tesla transformer. Actual measurement for R_1 and L_{k1} is necessary for further analysis.

The inductances and resistances of primary and secondary windings were measured by an Agilent 4263B digital electric bridge with the frequency of 100 kHz. The results are shown in Table II.

As shown in Fig. 1, the circuit formed by capacitance C_1, inductance $L_1 + L_{k1}$, and resistance R_1 was a second-order

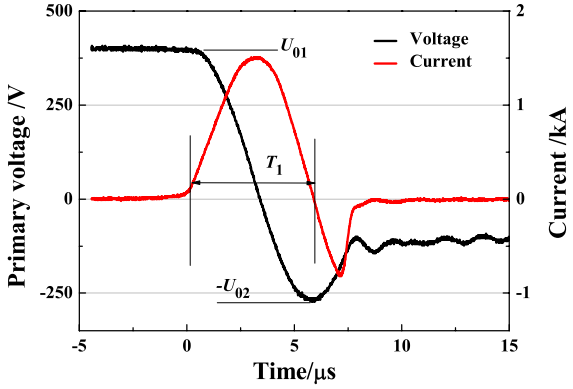

Fig. 9. Waveforms of primary voltage $u_1(t)$ with opened secondary circuit.

TABLE III
THEORETICAL VALUES OF SOME PARAMETERS

k_{eff}	n_{eff}	V	$\delta_{\max}$	T (μs)	$t_{\max}$ (μs)	λ
0.41	220	0.5	1.7	27.03	6.48	145

under-damped oscillation circuit when the secondary circuit was opened. The voltage across the capacitance C_1 has been shown in Fig. 9, among which $T_1 = 5.6$ μs, $U_{01} = 400$ V, and $U_{02} = 280$ V. The formula proposed by [15] to calculate R_1 and L_{k1} are as follows:

$$L_{k1} \approx \frac{T_1^2}{4\pi^2 C_1} - L_1 \tag{26}$$

$$R_1 \approx \frac{(L_1 + L_{k1})}{T_1} \ln\left(\frac{U_{01}}{U_{02}}\right). \tag{27}$$

And then, from the above equations, it can be obtained that $L_{k1} = 196.36$ nH, $R_1 = 36.93$ mΩ.

When the above parameters have been known, the theoretical value of parameters k_{eff}, n_{eff}, V, $\delta_{\max}$, T, $t_{\max}$, and λ can be calculated at the state of dual resonance according to (5), (15), (16), and (19). The results have been shown in Table III.

The experimental results show that the transformation rates changed from nearly 100 to 130 at different states and were all less than the theoretical calculation value 145. The reason is that the theoretical value of λ was calculated according to the free oscillation of the primary current. However, Fig. 5 shows that the primary current will be cut off when the thyristor was turn-off. The second peak value of u_2 in Fig. 4 did not reach its theoretical maximum value actually. Therefore, theoretical value calculated by the second peak became larger than the actual one.

The theoretical calculations of the parameters in Table III were all much affected by the stray inductance L_{k1} and resistance R_1. Moreover, the transformation ratio λ was much less than turns ratio ($N_2/N_1 = 480$), which clearly shows the influence from stray inductance L_{k1} and resistance R_1 on λ. Therefore, the value of primary resistance R_1 and stray inductance L_{k1} should be reduced as little as possible in the design of a Tesla transformer.

Unlike the magnetic core transformer, Tesla transformer did not suffer from core saturation. As shown in the foregoing analysis, so long as improving C_1 or U_1, the higher

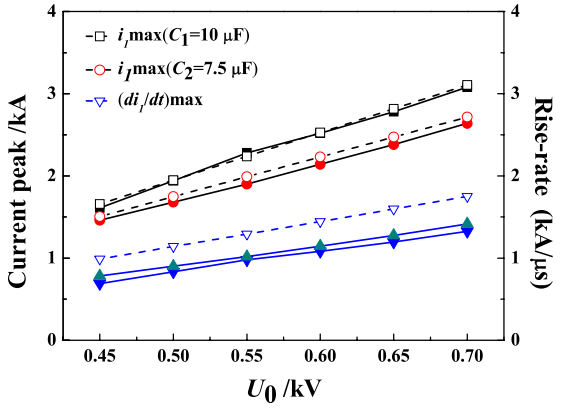

Fig. 10. Comparison between calculated values and test data of primary current peak and its rise-rate with different U_0 and C_1. (The calculated values and test data are represented by dashed lines and solid lines, respectively. The test data are the same as those in Fig. 8).

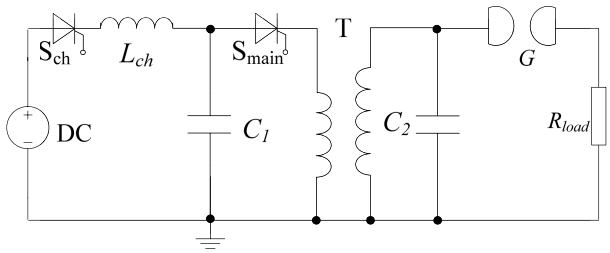

Fig. 11. Circuit for repetitive nanosecond pulse generating.

output transformation rate and voltage will be achieved due to increasing the primary magnetizing current. However, this may lead to exceeding the current specification of a semiconductor switch. The maximum value of the primary current $(i_1)_{\max}$ and its rise-rate $(di_1/dt)_{\max}$ should be estimated precisely based on the circuit parameters.

To get the values of $(i_1)_{\max}$ and $(di_1/dt)_{\max}$ under any charging voltage U_0, the key parameters γ and η in (24) and (25) should be calculated first. When the parameters L_{k1} and k_{eff} have to be measured and calculated, the theoretical results $\gamma_0 = 1.834$ and $\eta_0 = 4.05$ can be derived by (22) and (23). In contrast, Fig. 10 gives both the calculated values and the test data of $(i_1)_{\max}$ and $(di_1/dt)_{\max}$ with different U_0 and C_1. There are three dashed lines in Fig. 10 because the calculated values of $(di_1/dt)_{\max}$ have nothing to do with the C_1 theoretically. Fig. 10 shows that the calculated values of $(i_1)_{\max}$ are close to its test data while the calculated values of $(di_1/dt)_{\max}$ are significantly greater than its test data. The main reason is that the precise $(i_1)_{\max}$ was easily read through an oscilloscope while $(di_1/dt)_{\max}$ cannot be measured directly. The large error will be introduced in the calculating process of $(di_1/dt)_{\max}$ reference to the method in the literature [22], because it is difficult that the current starting points were exactly confirmed. To ensure reliability, it is proposed that the fast thyristor of primary circuit in Tesla transformer should be selected by theoretical value according to (22) and (23).

IV. High-Voltage Repetitive Nanosecond Pulse Generator

Utilizing a sharpening switch after secondary capacitance, the Tesla transformer can easily generate nanosecond pulses

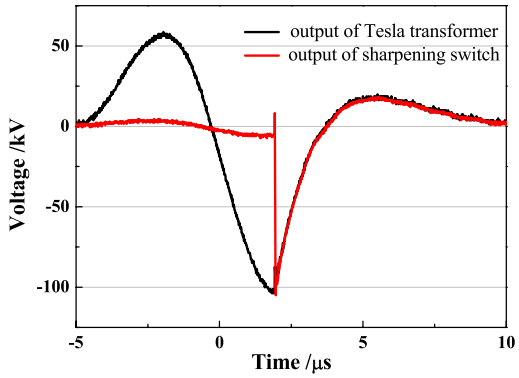

Fig. 12. Single nanosecond pulse waveform generated by sharpening switch.

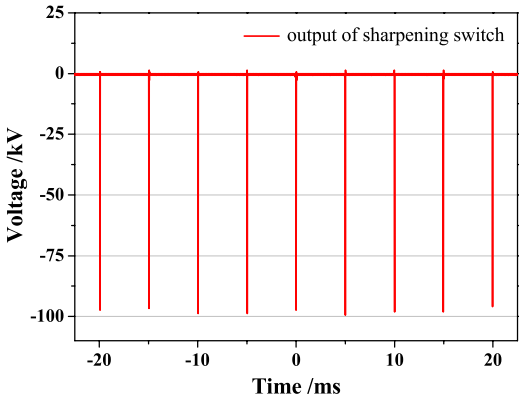

Fig. 13. Waveform of a series of nanosecond pulses at 200 Hz repetition rate.

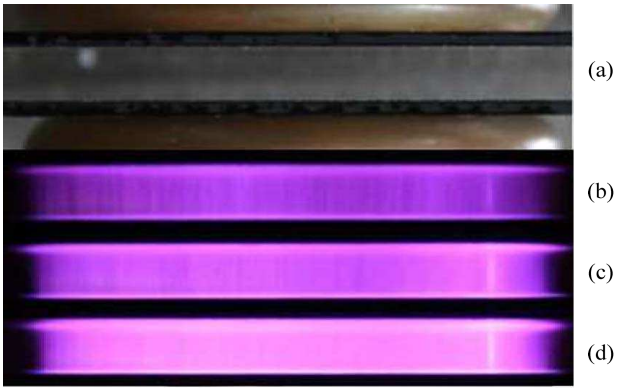

Fig. 14. Typical images of DBD in atmospheric air due to nanosecond pulses with different repetition rates. (a) Double-barrier parallel plate-plate electrodes. (b) Repetition rate of 50 Hz. (c) Repetition rate of 100 Hz. (d) Repetition rate of 200 Hz.

with hundreds of kilovolts. The circuit of nanosecond pulse generating has been shown in Fig. 11. An enclosed nitrogen-insulated two-electrode spark gap G was chosen as the sharpening switch. S_{ch} and L_{ch} are, respectively, charging thyristor and inductance. When $R_{\text{load}} = 6.0\ \text{k}\Omega$, the nanosecond pulse waveform across R_{load} by a resistive divider was shown as in Fig. 12. The output pulse of the sharpening switch is nearly 100 kV in peak, and 40 ns at the rise time (10%–90% points). When S_{ch} and S_{main} were alternately triggered by sequential control signal, the nanosecond pulse in Fig. 12 can be repetitively delivered to the load. Fig. 13 shows that the device based on the circuit in Fig. 11 can operate

at the repetition rate of 200 Hz. It can be observed that the peak power of the device is up to 1.67 MW and the average power, which equals to the peak power multiplied by the duty ratio, is only 232 W. The average power of pulse generator, which is very important for some application, increases with the repetition rate. Further improvement of the repetitive rate of the device depends on the modification of the charging circuit and the sharpening switch.

With the fast rise time, short pulse duration, and high repetition rate, the repetitive nanosecond pulses can be used to generate the atmospheric air nonequilibrium plasma. Fig. 14 shows the typical images of DBD in a standard atmospheric air due to the nanosecond pulses supplied with the developed pulse generator. With the increasing of the repetition rate, the homogeneous discharge is formed at the atmospheric air, which is necessary for a lot of practical applications.

V. Conclusion

A small-size spiral Tesla transformer has been developed. Based on this, the emphasis of this paper lies on the resonant charging characteristics of Tesla transformer. The contributions of this paper include the following.

1) The mathematical expressions for some key performances, e.g., secondary voltage, transformation ratio, primary current, and its rise-rate, were deuced. Primary resistance and stray inductance have large influence on the secondary voltage, and they should be reduced as little as possible in designing and fabricating. The transformation rate can be improved by increasing the detuning coefficient, or by increasing the primary capacitance.
2) The peak value of primary current is proportional to the square root of primary capacitance, while inversely to the total primary inductance. The maximum rise-rate of primary current is mainly determined by the total primary inductance. The semiconductor switch used in the primary circuit should be selected by theoretical calculation value according to relevant expression.
3) Compared with magnetic core transformer, the spiral Tesla transformer can easily realize the repetitive nanosecond pulse with smaller size and lighter weight. For ensuring resonant demand, the secondary capacitance of Tesla transformer with a high-voltage ratio has to be small. This means that the loading capacity is weak, which should be taken into consideration in the application of Tesla transformer.

References

[1] S. Furuya, T. Isiguro, T. Yoshida, S. Takano, and J. Irisawa, "Characteristics of flat-top nanosecond-pulse breakdown of gas-insulated gaps," in *Proc. 13th Int. Conf. High-Power Particle Beams*, 2000, pp. 591–594.

[2] T. Shao, G. Sun, P. Yan, and S. Zhang, "Breakdown phenomena in nitrogen due to repetitive nanosecond-pulse," *IEEE Trans. Dielectr. Electr. Insul.*, vol. 14, no. 4, pp. 813–819, Aug. 2007.

[3] L. Zhao, G.-Z. Liu, J.-C. Su, Y.-F. Pan, and X.-B. Zhang, "Investigation of thickness effect on electric breakdown strength of polymers under nanosecond pulses," *IEEE Trans. Plasma Sci.*, vol. 39, no. 7, pp. 1613–1618, Jul. 2011.

[4] E. I. Moses, "The national ignition facility and the national ignition campaign," *IEEE Trans. Plasma Sci.*, vol. 38, no. 4, pp. 684–689, Apr. 2010.

[5] V. P. Gubanov, S. D. Korovin, and I. V. Pegel, "Compact 1000 PPS high-voltage nanosecond pulse generator," *IEEE Trans. Plasma Sci.*, vol. 25, no. 2, pp. 258–265, Apr. 2011.

[6] A. Fridman, A. Chirokov, and A. Gutsol, "Non-thermal atmospheric pressure discharges," *J. Phys. D, Appl. Phys.*, vol. 38, no. 2, pp. R1–R24, 2005.

[7] Z. Cheng, S. Tao, L. Kaihua, Y. Yang, W. Jue, Z. Dongdong, *et al.*, "Surface treatment of polyethylene terephthalate films using DBD excited by repetitive unipolar nanosecond pulses in air at atmospheric pressure," *IEEE Trans. Plasma Sci.*, vol. 38, no. 6, pp. 1517–1526, Jun. 2010.

[8] S. O. Macheret, M. N. Shneider, and R. B. Miles, "Modeling of air plasma generation by repetitive high-voltage nanosecond pulses," *IEEE Trans. Plasma Sci.*, vol. 30, no. 3, pp. 1301–1314, Jun. 2002.

[9] F. Fukawa, N. Shimomura, and T. Yano, "Application of nanosecond pulse power to ozone production by streamer corona," *IEEE Trans. Plasma Sci.*, vol. 36, no. 5, pp. 2592–2597, Oct. 2008.

[10] G. A. Mesyats, S. D. Korovin, and V. V. Rostov, "The RADAN series of compact pulsed power generators and their applications," *Proc. IEEE*, vol. 92, no. 7, pp. 1166–1179, Jul. 2004.

[11] J. R. Reed, "Designing triple resonance Tesla transformers of arbitrary modal frequency ratio," *Rev. Sci. Instrum.*, vol. 77, no. 3, pp. 1–6, Mar. 2006.

[12] P. M. Ranon, "Compact pulsed transformer power conditioning system for generating high voltage, high energy, rapid rise time pulses," *IEEE Trans. Magn.*, vol. 25, no. 1, pp. 480–484, Jan. 1989.

[13] P. Sarkar, S. W. Braidwood, I. R. Smith, B. M. Novac, R. A. Miller, and R. M. Craven, "A compact battery-powered half-megavolt transformer system for EMP generation," *IEEE Trans. Plasama Sci.*, vol. 34, no. 5, pp. 1832–1837, Oct. 2006.

[14] K. K. Jain and P. W. Smith, "Fast-rise-time pulse transformers built from rotated stacked 1:1 transformers," *IEEE Trans. Plasma Sci.*, vol. 34, no. 5, pp. 1853–1858, May 2006.

[15] Z. Zhang, L. Zhang, Z. Meng, D. Li, S. Wang, Y. Cao, *et al.* "Experimental studies on a repetitive pulsed power modulator with a compact tesla transformer," in *Proc. 17th Int. Conf. High Power Particle Beams*, Jul. 2008, pp. 6–11.

[16] X. Jiaqi, L. Mingjia, and K. Qiang, "High transformer ratio and conical spiral air-cored pulse transformer," *High Power Laser Particle Beams*, vol. 22, no. 1, pp. 216–220, 2010.

[17] S. Xiao-xin, L. Guo-zhi, P. Jian-chang, S. Jian-cang, W. Li-min, Z. Xiao-xin, *et al.*, "A repetitive high-current pulsed accelerator—TPG700," in *Proc. 17th Int. Conf. High Power Particle Beams*, 2008, pp. 1–5.

[18] L. Mingjia, X. Jiaqi, K. Qiang, G. Shenggang, and J. Xiao "Development of 800 kV spiral air-cored transformer with high turn ratio," *High Power Laser Particle Beams*, vol. 23, no. 3, pp. 841–844, 2011.

[19] I. V. Romanchenko, V. V. Rostov, V. P. Gubanov, A. S. Stepchenko, A. V. Gunin, and I. K. Kurkan "Repetitive sub-gigawatt RF source based on gyromagnetic nonlinear transmission line," *Rev. Sci. Instrum.*, vol. 83, no. 7, pp. 074705-1–074705-6, Jul. 2012.

[20] E. M. M. Cost, "Resonance on coils excited by square waves: Explaining Tesla transformer," *IEEE Trans. Magn.*, vol. 46, no. 5, pp. 1186–1192, May 2010.

[21] G. A. Mesyats, S. D. Korovin, A. V. Gunin, V. P. Gubanov, A. S. Stepchenko, D. M. Grishin, *et al.*, "Repetitively pulsed high current accelerators with transformer charging of forming lines," *Laser Particle Beams*, vol. 21, no. 2, pp. 197–209, Apr. 2003.

[22] L. Li, C. Bao, X. Feng, Y. Liu, and L. Fochan, "Fast switching thyristor applied in nanosecond-pulse high-voltage generator with closed transformer core," *Rev. Sci. Instrum.*, vol. 84, no. 2, pp. 024703-1–024703-7, 2013.

Yunlong Liu was born in Gansu, China, in 1989. He received the B.S. degree from the College of Electrical Engineering, Xi'an Jiaotong University, Xi'an, China, in 2012. He is currently pursuing the master's degree with the High Voltage Engineering Department, Huazhong University of Science and Technology, Wuhan, China.

Li Lee was born in Hubei, China, in 1976. He received the Ph.D. degree from the Department of Electronics and Information Engineering, Huazhong University of Science and Technology (HUST), Wuhan, China, in 2006.

He is currently an Associate Professor with the State Key Laboratory of Advanced Electromagnetic Engineering and Technology, HUST.

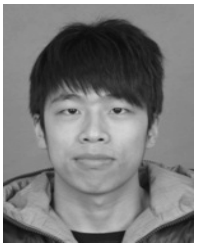

Yu Bing was born in Zhejiang, China, in 1990. He received the B.S. degree from the College of Electrical and Electronic Engineering, Huazhong University of Science and Technology (HUST), Wuhan, China, in 2012, where he is currently pursuing the master's degree with the High Voltage Engineering Department.

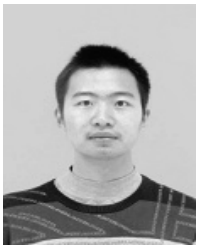

Yafeng Ge was born in Anhui, China, in 1990. He received the B.S. degree from the China University of Petroleum, Beijing, China, in 2012. He is currently pursuing the master's degree with the High Voltage Engineering Department, Huazhong University of Science and Technology, Wuhan, China.

Wen Hu was born in Hubei, China, in 1991. She received the B.E. degree from the College of Electrical and Electronic engineering, Hubei University of Technology, Wuhan, China, in 2013, where she is currently pursuing the master's degree with the High Voltage Engineering Department

Fuchan Lin was born in Zhejiang, China, in 1969. He received the Ph.D. degree from the College of Electrical and Electronic Engineering, Huazhong University of Science and Technology (HUST), Wuhan, China, in 1996.

He is currently a Professor with the College of Electrical and Electronic Engineering, HUST. He has been involved in research on pulsed power technology.